

Radiation Damage and Dimensional Changes

A. A. El-Barbary, H. I. Lebda and M. A. Kamel

Physics department, Faculty of Education, Ain-Shams University, Roxy, Cairo, Egypt

ahla_eg@yahoo.co.uk

ABSTRACT

The dimensional changes have been modeled in order to be accommodated in the reactor design. This study has major implications for the interpretation of damage in carbon based nuclear fission and fusion plant materials. Radiation damage of graphite leads to self-interstitials and vacancies defects. The aggregation of these defects causes dimensional changes. Vacancies aggregate into lines and disks which heal and contract the basal planes. Interstitials aggregate into interlayer disks which expand the dimension

Key Words: Radiation Damage, Irradiated Graphite, Vacancy Defects, Dimensional Changes

INTRODUCTION

Dimensional changes were the earliest and most obvious observations in irradiated graphite(1). Expanding in the direction perpendicular to the basal planes (along *c*-axis) and contracting in the direction parallel to them were observed. Graphite is used as a moderator in the nuclear reactor. For nuclear design, the determination of the dimensional changes due to the bombardment with neutrons is very important. The irradiation damage is dependent on the degree of perfection of crystals: the less perfection the more damage(1). In nuclear graphite, crystallites in the polycrystalline material can grow anisotropically at different rates and directions, resulting in an increase of the internal stresses at the crystallites boundaries. Within the bulk, irradiation with ions or neutrons creates a cascade of Frenkel pairs which are thought to reorganise into vacancy lines and interstitial loops. There are two measures of the dimensional changes in bulk graphite. First, the changes in the lattice parameters, Δa and Δc , parallel and perpendicular to the basal plane. Second, the changes in the crystal dimensions, ΔX_a and ΔX_c . The relations between them are found to be,

$$\Delta X_a / X_a \geq \Delta a / a \quad \dots\dots\dots[1]$$

and

$$\Delta X_c / X_c \geq \Delta c / c \quad \dots\dots\dots[2]$$

These relations are dependent on the type of defects in graphite. The changes in the crystal dimensions can exceed the changes in the lattice parameters ($\Delta X_a / X_a > \Delta a / a$, and $\Delta X_c / X_c > \Delta c / c$) when vacancy lines collapse and extra interstitial planes start to form(1).

METHODS

Now we turn to our first principles calculations of the dimensional changes. We took a supercell of a graphene sheet, C_{144} , and inserted vacancies in lines of different orientation and discs. Although interlayer interactions are missing, corresponding energies are of the order of 0.035 eV/atom(2) are small compared with the energies we found. The calculations were

performed using LDA within DFT. The many-body wavefunctions were constructed from a tempered set of 4 radial Gaussians per atom, modified by s and p spherical harmonics (the second smallest Gaussian is augmented by a set of d functions). BZ sampling is performed using 1 x 2 x 1 k-points generated using the Monkhorst and Pack algorithm(3).

RESULTS, DISCUSSION and CONCLUSION

Both STM and EM have been used to investigate dislocations in graphite. EM can detect the dislocations anywhere, at surface or in bulk. STM can only image the dislocations close to the surface, otherwise the dislocations will not be detected. However, the advantage of the STM is its ability of distinguishing between the disc vacancy and the interstitial loops. The latter appear as bumps and the former as depressions in STM. Both the vacancy and interstitial loops are detected as dark and bright regions, respectively, in graphite samples using STM(4). The depth and height of the vacancy and interstitial loops were found to be 2.8 Å, and 3.0 Å, respectively.

Figure (1) shows the atoms removed and the equivalent dislocations for V_2^1 , V_4^b , V_6^b , V_4^z , and V_6^z vacancies: *b* and *z* referring to the boat $\langle 01\bar{1}0 \rangle$ and zigzag $\langle 2\bar{1}\bar{1}0 \rangle$ directions. *L* and *h* are the basal dimensions of the C_{144} supercell, and are equal to 25.40 Å, and 14.64 Å, respectively. The distance between the dislocations in the dipole (*W*) is represented as a black line in each box, and the Burgers vector (\underline{b}) as a blue line within the same box. (**T**) is placed at the dislocation position. The Burgers vector is equal to the lattice parameter for the zig-zag vacancy lines, ($\underline{b}=a$), and to the half of the lattice parameter for the boat vacancy lines, ($\underline{b}= \frac{1}{2}a$). Table (1) shows the basal contraction calculations (ΔXa) for the boat and zig-zag vacancy clusters in graphite, using the following formulae(5).

$$\begin{array}{lll} \underline{b} W/L & \text{for boat vacancy lines} & \dots\dots[3] \\ \underline{b} W/h & \text{for zig-zag vacancy lines} & \dots\dots[4] \end{array}$$

The dimensional changes (ΔXa) under complete healing are calculated using formulae [3] and [4] for the boat and zig-zag vacancies lines, respectively. The results are shown in Table (1). The basal contractions for V_2^1 , V_4^b (V_4^z) and V_6^b (V_6^z) are -0.21 Å, -0.41 Å (-0.71 Å) and -0.62 Å (-1.07 Å), respectively. The calculated formation areas are -5.24 Å², -10.48 Å² (-10.48 Å²) and -15.72 Å² (-15.72 Å²), respectively, for V_2^1 , V_4^b (V_4^z) and V_6^b (V_6^z). The atomic areas are 2, 4 (4) and 6 (6) for V_2^1 , V_4^b (V_4^z) and V_6^b (V_6^z), respectively.

After the formation areas (ΔA_v) and the atomic areas ($\Delta A_v/A_{atom}$) for the boat and zig-zag vacancy lines are determined, their volume changes (ΔV) and their atomic volumes ($\Delta V_v/V_{atom}$) are calculated then. The calculations of the volume changes, assuming complete healing for the collapsed boat and zig-zag vacancy lines are shown in Table (1). The calculated volume contractions of V_2^1 , V_4^b (V_4^z) and V_6^b (V_6^z) are -17.56 Å³, -35.11 Å³ (-35.11 Å³) and -52.67 Å³ (-52.67 Å³), respectively. The atomic volumes ($\Delta V_v/V_{atom}$) are 2, 4 (4), and 6 respectively, for V_2^1 , V_4^b (V_4^z) and V_6^b (V_6^z). The basal contractions were also investigated by first principles calculations. Our first principles calculations of the basal contractions for the boat and zig-zag vacancy clusters are performed by independent optimisation of the lattice vectors along *h* and *L* directions, respectively, while their geometries are fully relaxed. The results are shown in Table (2). The basal contractions for

V_2^1 , V_4^b (V_4^z) and V_6^b (V_6^z) are -0.14 \AA , -0.31 \AA (-0.61 \AA), and -0.46 \AA , (-0.86 \AA), respectively. The calculated formation areas are -3.60 \AA^2 , -7.87 \AA^2 , (-8.93 \AA^2), and -11.68 \AA^2 (-12.62 \AA^2), and the atomic areas are 1.36, 3.00 (3.41) and 4.46 (4.82) for V_2^1 , V_4^b (V_4^z) and V_6^b (V_6^z), respectively. Table (2) shows also the first principles calculations of the volume changes for the boat and zig-zag vacancy clusters in graphite. The volume contractions for V_2^1 , V_4^b (V_4^z) and V_6^b (V_6^z) are -11.93 \AA^3 , -26.36 \AA^3 (-29.92 \AA^3), and -39.13 \AA^3 (-42.28 \AA^3), respectively. The atomic volumes are 1.36, 3.00 (3.41) and 4.46 (4.82) for V_2^1 , V_4^b (V_4^z) and V_6^b (V_6^z), respectively.

It is clear that both type of collapsed vacancy lines (boat and zig-zag) can cause basal contractions and that basal contractions via the relaxed vacancies are always less than the basal contractions via the complete healing estimations. This observation can be explained/confirmed through the calculated formation energy of vacancy types. We have reported that the formation energies of the mono-vacancy and di-vacancy are 8.44 eV and 8.25 eV, respectively, and here we have found that the atomic area ($\Delta A_v/A_{\text{atom}}$) of the di-vacancy (V_2^1) is 1.36 (i.e. close to the complete healing of the mono-vacancy). Therefore, the reaction $V+V \rightarrow V_2^1$ leads to an energy and a basal area change reasonably consistent with "disappearance" of a vacancy. It is expected that increasing the size of the vacancy lines leads to an increase in the basal contraction, which is confirmed by our calculations. The reactions $V_2^1+V_2^1 \rightarrow V_4^b$ (V_4^z) and V_4^b (V_4^z) + $V_2^1 \rightarrow V_6^b$ (V_6^z) are found to be accompanied with basal contraction larger than the basal contraction via their individual V_2^1 vacancies.

There is not any previous work on the basal dimensional changes of graphite at atomic level that can be used for a quantitative comparison. Our calculations are consistent with the experimental observation of the contraction along the basal plane using TEM diffraction(6). The basal contraction has been studied at macroscopic level using kinetic irradiation models(7-8). Horner *et al.* (8) has developed the Woolley kinetic model. Their model can account for the random formation of the vacancy complexes, allow the nucleation of the interstitial clusters and the annihilation of interstitials at vacancies and give estimates of the density of the various defects. In their model, di-vacancies were considered as line nuclei and each line was considered as having a "sink" at each end where newly formed vacancies may be absorbed. They have concluded that the most probable way to add a mono-vacancy is that which extends the "line" produced by the di-vacancy. Their model suggests that if the line defects collapse to nearly heal the lattice, it is difficult to anneal away. Their suggestion was supported by experimental evidence on the annealing of heavily damaged materials up to 2500 °C, where large interstitial clusters remained. It was explained as the net interstitial population which results from formation of the vacancy lines which are difficult to anneal. The evidence we have here is that vacancy healing is very effective. To conclude, for the first time we have estimated the basal contraction for vacancy lines at atomic level. The atomic volumes are found to be 1.36, 3.00 (3.41) and 4.46 (4.82) for V_2^1 , V_4^b (V_4^z) and V_6^b (V_6^z), respectively. These values appear consistent with very effective "healing", and thus with the low formation energy of vacancy lines.

REFERENCES

- (1) Chemistry and Physics of Carbon, ed. P. L. Walker, vol. 2 (Edward Arnold, London 1966)
- (2) R. H. Telling and M. I. Heggie, *Phil. Mag. Lett.* **83**, 411 (2003).
- (3) H. J. Monkhorst and J. D. Pack, *Phys. Rev. B* **13**, 5188 (1976), P. R. Briddon and R. Jones, *Phys. Stat. Sol. b* **217**, 131 (2000), A. A. EL-Barbary, R. H. Telling, C. P. Ewels, M. I. Heggie, *Phys. Rev. B.* **68**, 144107 (2003), C. P. Ewels, R. H. Telling, A. A. EL- Barbary, M. I. Heggie, *Phys. Rev. Lett.* **91**, 025505 (2003), R. H. Telling, C. P. Ewels, A. A. EL-Barbary, M. I. Heggie, *Nature Mater.* **2**, 333 (2003).
- (4) P. J. Ouseph, *Phys. Stat. Sol. a* **169**, 25 (1998).
- (5) N. Lehto and S.Oberg, *Phys. Rev. Lett.* **80**, 5568 (1998).
- (6) J. Koike and D. F. Pedraza, *J. Mater. Res.* **9**, 1899 (1994).
- (7) G. B. Neighbour, *J. Phys. D: Appl. Phys.* **33**, 2966 (2000).
- (8) P. Horner and G. K. Williamson, *Carbon* **4**, 353 (1966).

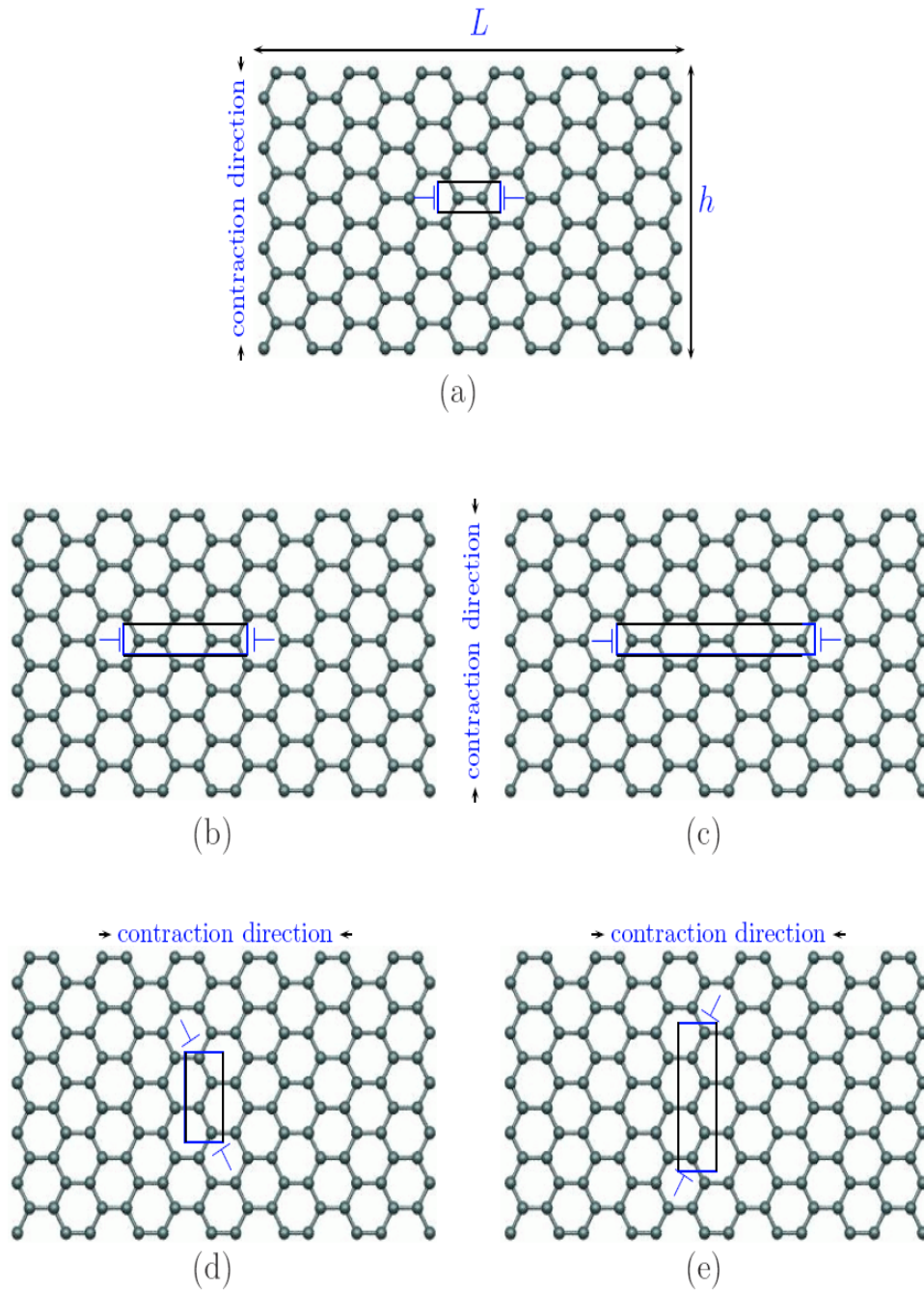


Fig (1) Schematic of atoms removed and equivalent dislocations for a) $V2L$, b) $V4b$, c) $V6b$, d) $V4Z$, and e) $V6Z$ vacancies. L and h are the basal dimensions of the C144 supercell and are equal to 25.40 Å and 14.64 Å, respectively. The distance between the dislocations in the dipole (W) is represented as a black line in each box, and the Burgers vector (b) as a blue line within the same box. (T) refers to the dislocation position.

TABLE I: The complete healing calculations along the basal plane, (ΔX_a), using the formulae and (4), the formation areas (ΔA_v) and the atomic areas ($\frac{\Delta A_v}{A_{atom}}$) for the boat and zig-zag vaca lines of graphite. The lattice parameter $a=2.46 \text{ \AA}$. The area per atom (A_{atom})= $\frac{\sqrt{3}a^2}{4}=2.62 \text{ \AA}^2$ the volume per atom (V_{atom})= 8.777 \AA^3 .

	ΔX_a	ΔA_v	ΔV_v	$\frac{\Delta A_v}{A_{atom}}$ $(\frac{\Delta V_v}{V_{atom}})$
V_2^1	$\underline{b}(\frac{W}{L}) = -\frac{1}{2} a (\frac{\sqrt{3}a}{6\sqrt{3}a}) = -\frac{1}{12}a = -0.21$	$L \Delta X_a = -\frac{\sqrt{3}}{2} a^2 = -5.42$	-17.56	2
V_4^b	$\underline{b}(\frac{W}{L}) = -\frac{1}{2} a (\frac{2\sqrt{3}a}{6\sqrt{3}a}) = -\frac{1}{6} a = -0.41$	$L \Delta X_a = -\sqrt{3} a^2 = -10.48$	-35.11	4
V_6^b	$\underline{b}(\frac{W}{L}) = -\frac{1}{2} a (\frac{3\sqrt{3}a}{6\sqrt{3}a}) = -\frac{1}{4} a = -0.62$	$L \Delta X_a = -\frac{3\sqrt{3}}{2} a^2 = -15.72$	-52.67	6
V_4^z	$\underline{b}(\frac{W}{h}) = -a (\frac{\sqrt{3}a}{6a}) = -\frac{\sqrt{3}}{6} a = -0.71$	$h \Delta X_a = -\sqrt{3} a^2 = -10.48$	-35.11	4
V_6^z	$\underline{b}(\frac{W}{h}) = -a (\frac{3\sqrt{3}a}{2(6a)}) = -\frac{\sqrt{3}}{4} a = -1.07$	$h \Delta X_a = -\frac{3\sqrt{3}}{2} a^2 = -15.72$	-52.67	6

TABLE II: First principles calculations of the basal contractions, (ΔX_a), the formation areas (ΔA_v) and the atomic areas ($\frac{\Delta A_v}{A_{atom}}$) of the boat and zig-zag vacancy clusters in graphite. The area per atom (A_{atom})= $\frac{\sqrt{3}a^2}{4}=2.62 \text{ \AA}^2$ and the volume per atom (V_{atom})= 8.777 \AA^3 .

	ΔX_a	ΔA_v	ΔV_v	$\frac{\Delta A_v}{A_{atom}}$ ($\frac{\Delta V_v}{V_{atom}}$)
V_2^1	-0.14	$L \Delta X_a = -3.60$	-11.93	1.36
V_4^b	-0.31	$L \Delta X_a = -7.87$	-26.36	3.00
V_6^b	-0.46	$L \Delta X_a = -11.68$	-39.13	4.46
V_4^z	-0.61	$h \Delta X_a = -8.93$	-29.92	3.41
V_6^z	-0.86	$h \Delta X_a = -12.62$	-42.28	4.82